Electronic Supplementary Material (ESI) for Journal of Materials Chemistry A.
This journal is © The Royal Society of Chemistry 2014

Supporting Information

One Pot Synthesis of Ultrasmall MoO_3 Nanoparticles Supported on SiO_2, TiO_2, and ZrO_2 Nanospheres: An Efficient Epoxidation Catalyst

Prakash Chandra, Dhananjay S. Doke, Shubhangi B. Umbarkar and Ankush V. Biradar

Catalysis Division, CSIR-National Chemical Laboratory, Dr. Homi Bhabha Road, Pune, 411008, Maharashtra, India.

E-mail: av.biradar@ncl.res.in, Fax: 020 2590 2633.

Contains:

S1: Details of instrument used for catalyst characterization

S2: Catalyst characterization by TEM

S3: Catalyst characterization by SEM for EDAX and metal mapping

S4: Catalyst characterization by XRD

S5: Catalyst characterization by Raman spectroscopy

S6: Catalyst surface area analysis by BET method

S7: Acidity measurement of catalysts by TPD method

S8: Catalyst characterization by XPS analysis

S9: Results of catalytic recycle studies

S10: TEM analysis of the spent catalyst

S11: Catalyst leaching studies by hot filtration Vs blank

S1: Details of instrument used for catalyst characterization

A. Powder X-ray analysis: X-ray diffractograms were recorded using a Rigaku X-ray diffractometer (Model DMAX IIIVC) using CuKa (1.5406 Å) radiation from $2\theta=20$ to 80º by 0.1º steps with an integration time of 4 s.

B. Raman analysis: Raman spectra were recorded under ambient conditions on a LabRAM infinity spectrometer (Horiba–Jobin–Yvon) equipped with a liquid nitrogen detector and a frequency doubled Nd-YAG laser supplying the excitation line at 532nm with 1–10mW power. The spectrometer is calibrated using the Si line at 521 cm^{-1} with a spectral resolution of 3 cm^{-1}.

D. Electron microscopy: Scanning electron microscopy (SEM) measurements were performed on a FEI quanta 200 3D dual beam (ESEM) having thermionic emission tungsten filament in the 3 nm range at 30 kV and HRTEM was done on a Tecnai G2-30 FEI instrument operating at an accelerating voltage of 300 kV. Before analysis, the powders were ultrasonically dispersed in isopropanol, and two drops of isopropanol containing the solid were deposited on a carbon coated copper grid.

E. FT-IR spectroscopy: The acidity of the samples was finely determined using pyridine adsorption by using a Shimadzu 8000 series FTIR spectrometer in the diffuse reflectance infrared Fourier transform (DRIFT) mode. As a pretreatment, the sample was placed in the DRIFT cell and heated to 400 °C under a flow of inert gas (N_2) for 2 h. After cooling to 100 °C, pyridine was introduced in an N_2 flow. The physisorbed pyridine fraction was first removed by flushing the cell with N_2 for 45 min, and the first spectrum was recorded. Then, pyridine was desorbed for 45 min at 100, 150, 200 and 300 °C and spectra were recorded at each temperature. The spectrum of the neat catalyst (before pyridine adsorption) at 100 °C was subtracted from all the spectra.

F. Acidity measurements: The NH_3-TPD experiments were performed using a Micromeritics Autochem 2910 instrument. A weighed amount of the sample (~100 mg) was placed in a quartz reactor, pretreated in a flow of He gas at 500 °C for 1h (ramp rate of $10Kmin^{-1}$) and cooled to 100 °C.The catalyst was then exposed to a gas mixture of NH_3 (5% NH_3–95% He, 50 $mLmin^{-1}$) at 100 °C, followed by evacuation at 100 °C for 3h.Then, the measurement was carried out from 100 °C to 500 °C with a heating rate of $5Kmin^{-1}$ in He as a carrier gas at a flow rate of 60 $mLmin^{-1}$ until ammonia was desorbed completely.

G. BET details: N_2 adsorption–desorption isotherms were recorded at 77 K by using an automated quantasorb instrument from quantachrome. Before each run, a known mass of sample (around 0.200 g) was heated at 200 °C under vacuum for 2.5 h. Specific surface areas were calculated from the linear part of the Brunauer–Emmett–Teller line. Pore-size distributions were obtained by applying the Barrett–Joyner–Halenda (BJH) equation to the desorption branch of the isotherm. The total pore volume was estimated from the N_2 uptake at a P/P_0 value of 0.991.

S2: Catalyst characterization by TEM

a) TEM images of TiO_2 nanoparticles synthesized by reverse micelle method

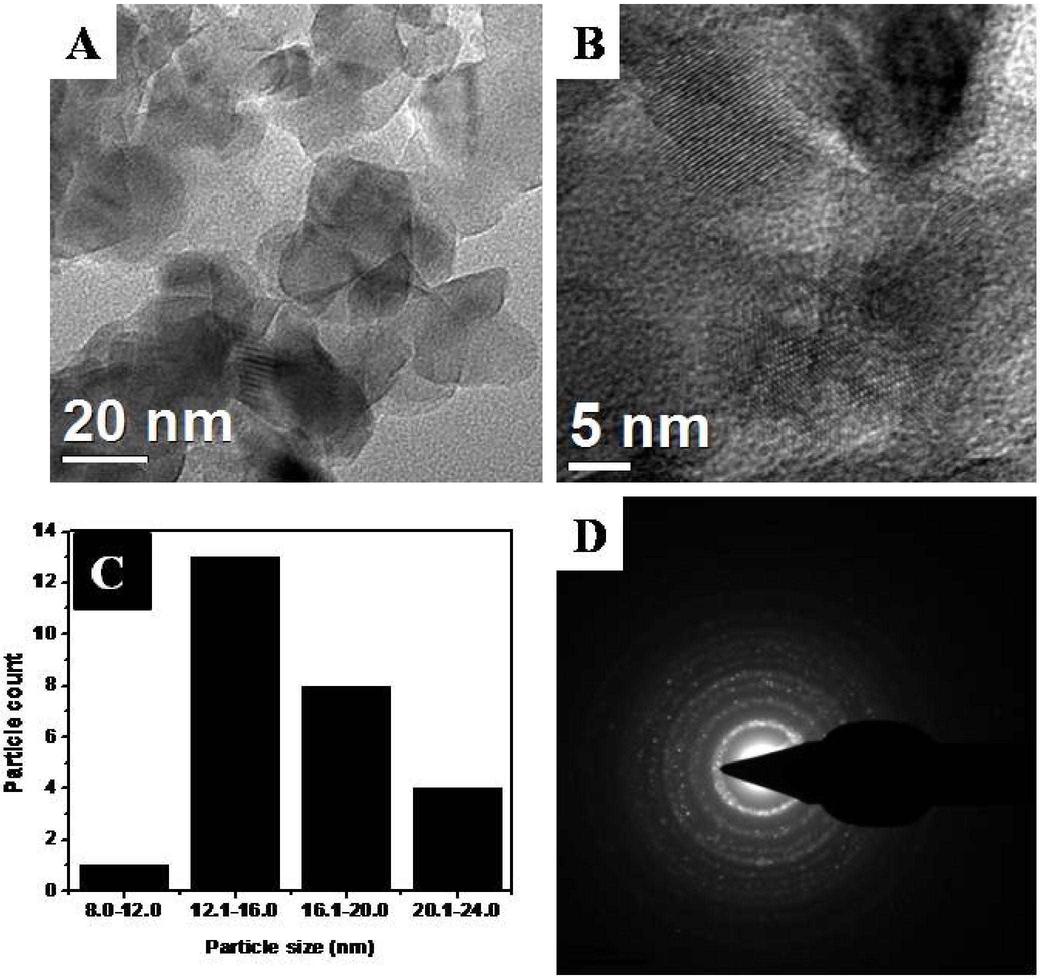

Fig S2-1: HRTEM image of TiO_2 at (A) 20 nm; (B) 5 nm scale; (C) Particle size distributions and (D) SAED image.

b) TEM images of ZrO_2 nanoparticles synthesized by reverse micelle method

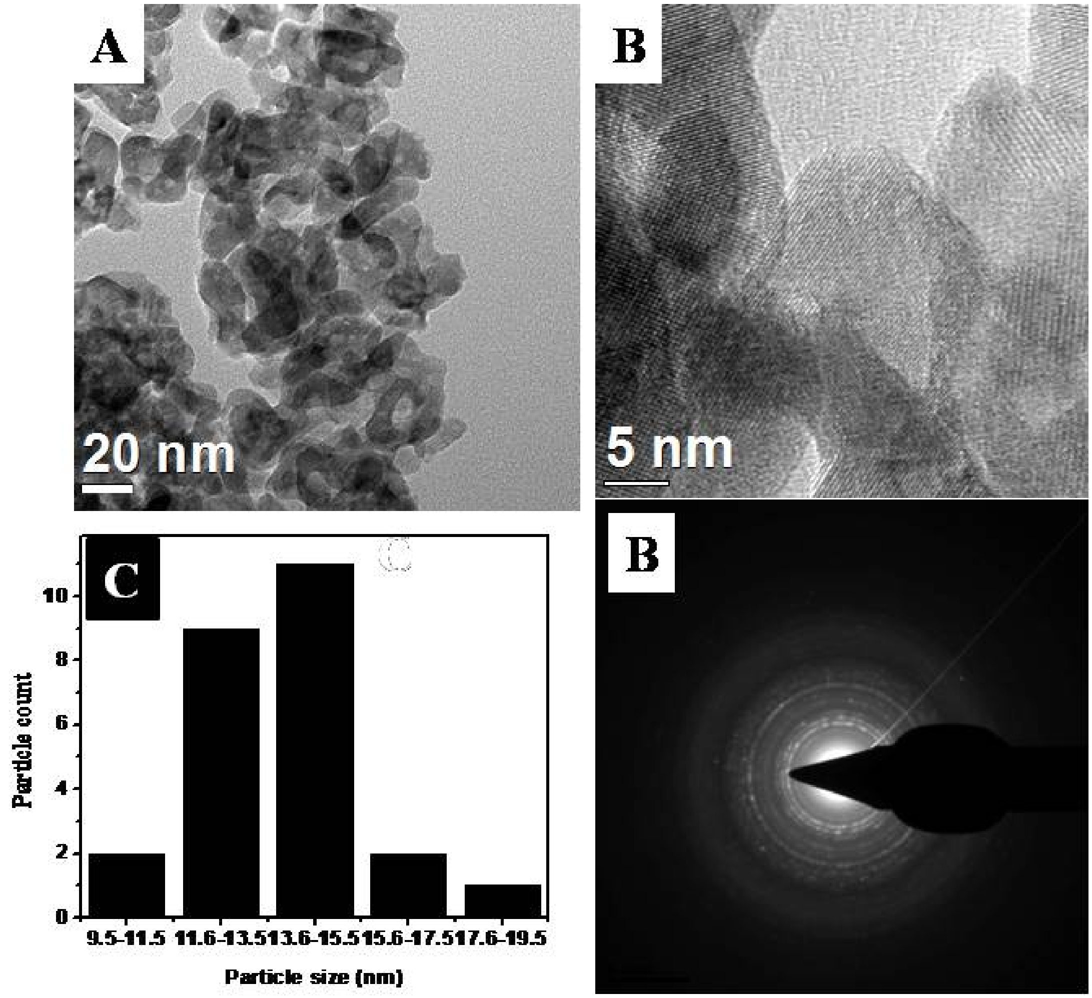

Fig S2-2: HRTEM image of ZrO_2 with ammonia at (A) 20 nm; (B) 5 nm scale; (C) Particle size distributions and (D) SAED image.

S3: Catalyst characterization by SEM for EDAX and metal mapping

a) SEM-EDAX analysis of MoO_3/SiO_2 nanospheres

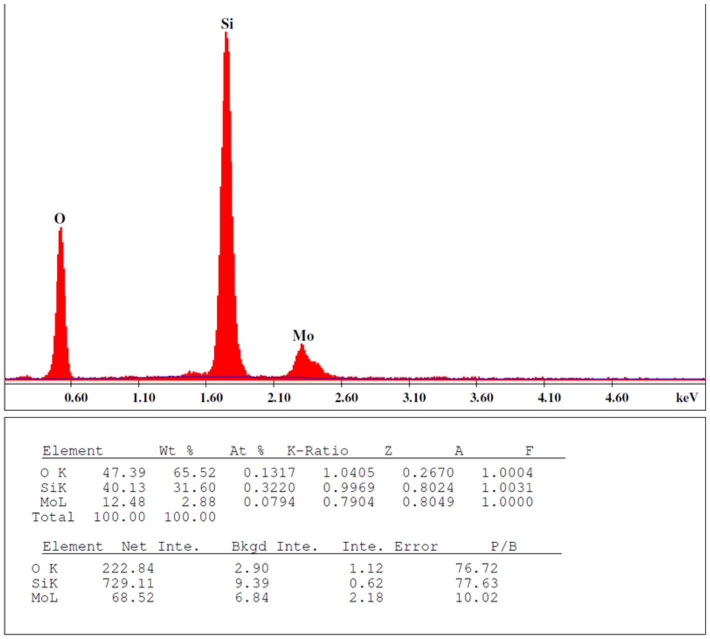

```
 Element       Wt %     At %   K-Ratio     Z         A         F
 O K     47.39    65.52   0.1317   1.0405   0.2670   1.0004
 SiK     40.13    31.60   0.3220   0.9969   0.8024   1.0031
 MoL     12.48     2.88   0.0794   0.7904   0.8049   1.0000
Total   100.00   100.00

 Element   Net Inte.     Bkgd Inte.    Inte. Error       P/B
O K      222.84          2.90          1.12          76.72
SiK      729.11          9.39          0.62          77.63
MoL       68.52          6.84          2.18          10.02
```

Fig S3-1: represents the SEM-EDAX of MoO_3/SiO_2 nanospheres

b) EDAX elemental mapping of the MoO_3/TiO_2 nanospheres

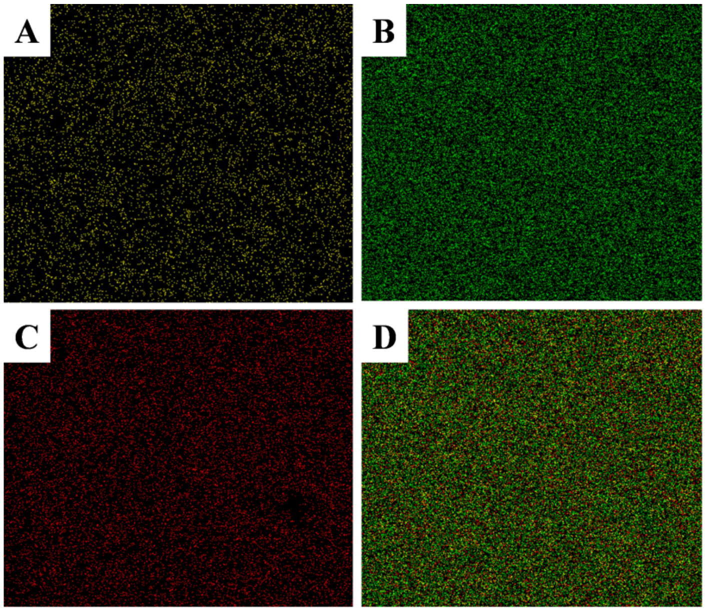

Fig S3-2: Showing elemental mapping of the MoO_3/TiO_2 nanospheres; (A) yellow color shows molybdenum atom; (B) green color shows titania atoms; (C) red color shows oxygen atoms present on surface and (D) MoO_3/TiO_2 on the surface.

c) SEM-EDAX analysis of MoO_3/TiO_2 nanospheres

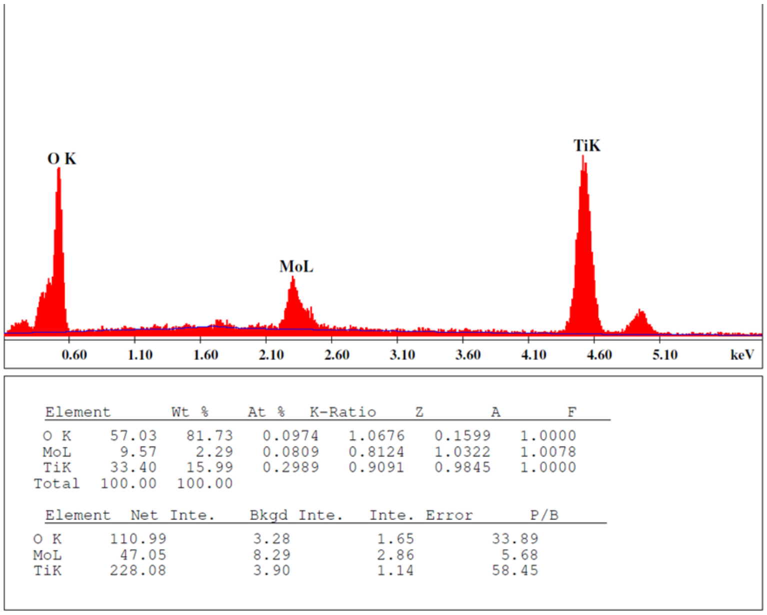

```
 Element         Wt %     At %   K-Ratio     Z         A        F
 O K     57.03    81.73    0.0974    1.0676    0.1599    1.0000
 MoL      9.57     2.29    0.0809    0.8124    1.0322    1.0078
 TiK     33.40    15.99    0.2989    0.9091    0.9845    1.0000
Total   100.00   100.00

 Element   Net Inte.    Bkgd Inte.    Inte. Error       P/B
O K       110.99         3.28          1.65           33.89
MoL        47.05         8.29          2.86            5.68
TiK       228.08         3.90          1.14           58.45
```

Fig S3-3: represents the SEM-EDAX pattern of MoO_3/TiO_2

d) EDAX elemental mapping of the MoO_3/ ZrO_2 nanospheres

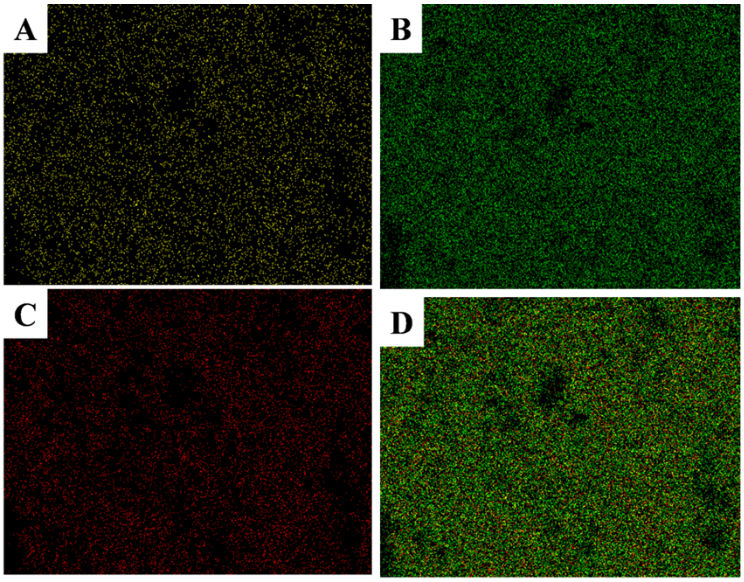

Fig S3-4: Showing elemental mapping of the MoO_3/ZrO_2 synthesized nanospheres; (A) yellow color shows molybdenum content; (B) green color shows zirconia atoms; (C) red color shows oxygen atoms present on surface and (D) MoO_3/ZrO_2 on the surface.

e) SEM-EDAX analysis of MoO_3/TiO_2 nanospheres

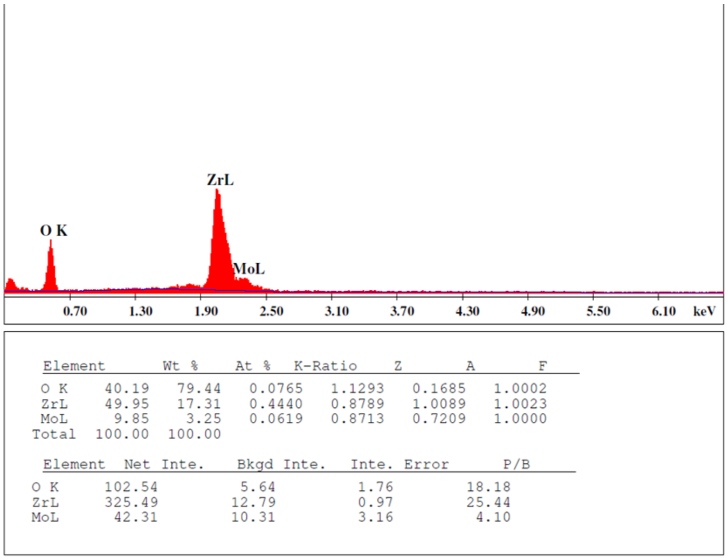

```
 Element        Wt %     At %   K-Ratio     Z        A        F
  O K    40.19   79.44   0.0765   1.1293   0.1685   1.0002
  ZrL    49.95   17.31   0.4440   0.8789   1.0089   1.0023
  MoL     9.85    3.25   0.0619   0.8713   0.7209   1.0000
 Total  100.00  100.00

 Element  Net Inte.    Bkgd Inte.   Inte. Error      P/B
 O K       102.54          5.64        1.76         18.18
 ZrL       325.49         12.79        0.97         25.44
 MoL        42.31         10.31        3.16          4.10
```

Fig S3-5: represents the SEM-EDAX of MoO_3/ZrO_2 nanospheres.

S4: Catalyst characterization by XRD

a) Powder XRD pattern of (a) titania; (b) MoO_3/TiO_2

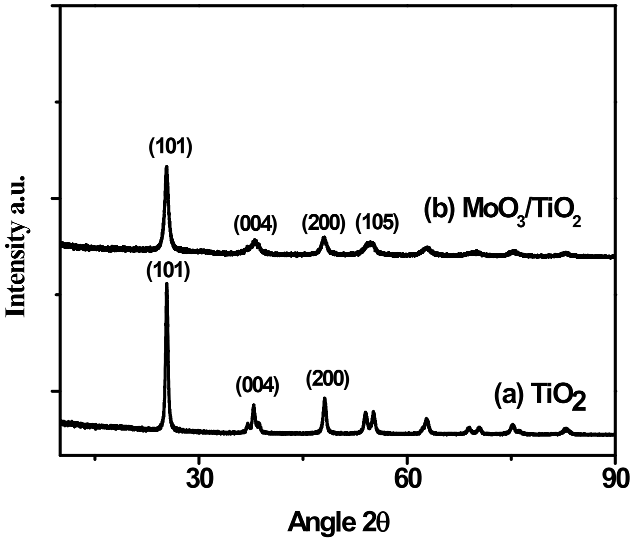

Fig S4-1: Powder XRD pattern of (a) titania; (b) MoO_3/TiO_2.

b) Powder XRD pattern (a) ZrO_2; (b) MoO_3/ ZrO_2

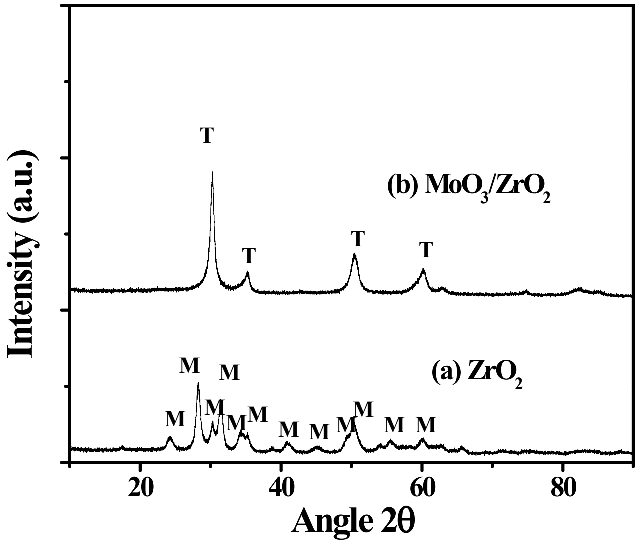

Fig S4-2: Powder XRD pattern (a) ZrO_2; (b) MoO_3/ ZrO_2.

S5 Catalyst characterization by Raman spectroscopy

a) Raman spectra of (A) (a) TiO_2 (b) MoO_3/TiO_2

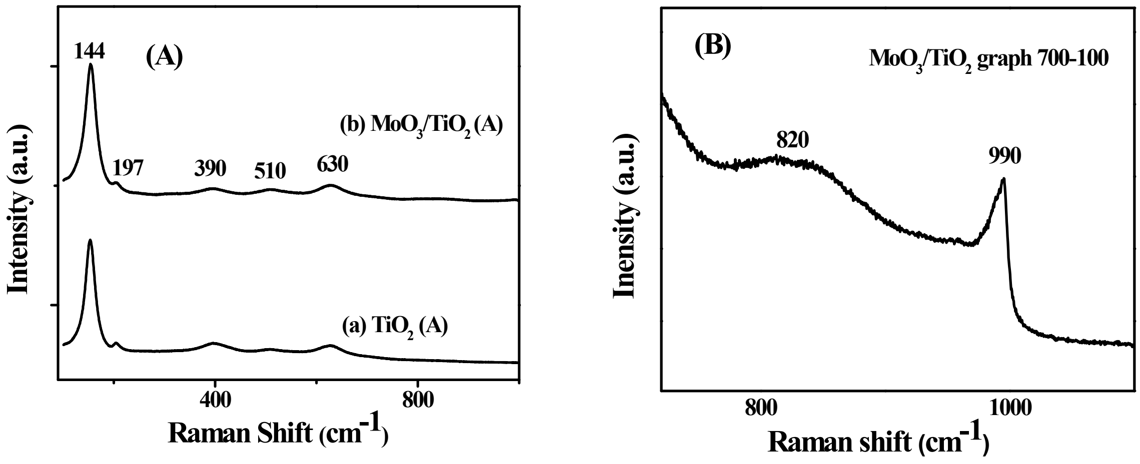

Fig. S5-1: Raman spectra of (A) (a) TiO_2 (b) MoO_3/TiO_2; (b) graph shows expanded view in range the 700 - 1200 cm^{-1} for MoO_3/TiO_2.

b) Raman spectra of (a) ZrO_2 (b) MoO_3/ZrO_2

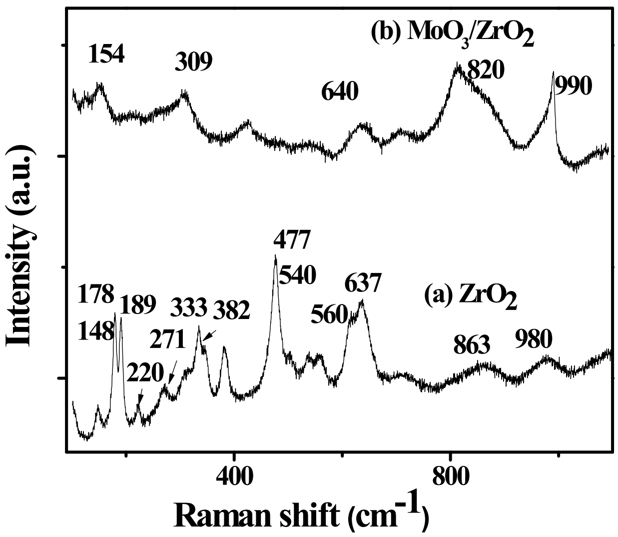

Fig. S5-2: Raman spectra of (a) ZrO_2 (b) MoO_3/ZrO_2.

S6- Catalyst surface area analysis by BET method

Table ST-1. Results of BET surface area of different catalysts

Catalyst	**BET surface area (m^2/g)**	**Pore volume (cm^3/g)**	**Pore size (Å)**
MoO_3/SiO_2	22.79	0.009982	33.4950
MoO_3/TiO_2	89.156	0.09281	20.8203
MoO_3/ZrO_2	139.679	0.009982	34.7939

a) BET surface area measurements of MoO_3/SiO_2; MoO_3/TiO_2; and MoO_3/ZrO_2

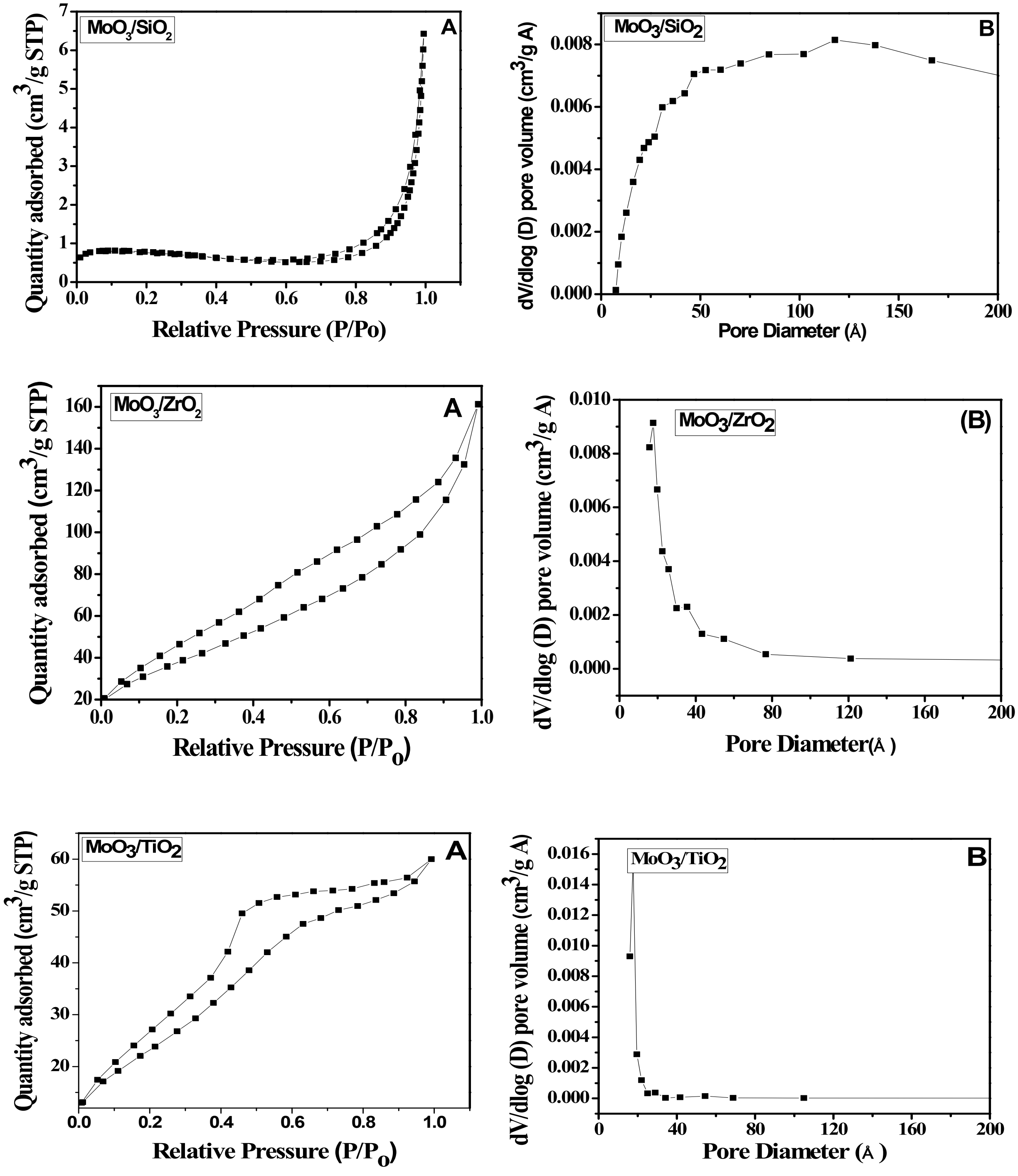

Fig.-S6-1: (A) BET surface area isotherms and (B) pore volume distribution curve for MoO_3/SiO_2; MoO_3/TiO_2; and MoO_3/ZrO_2

S7- Acidity measurement of catalysts by TPD method

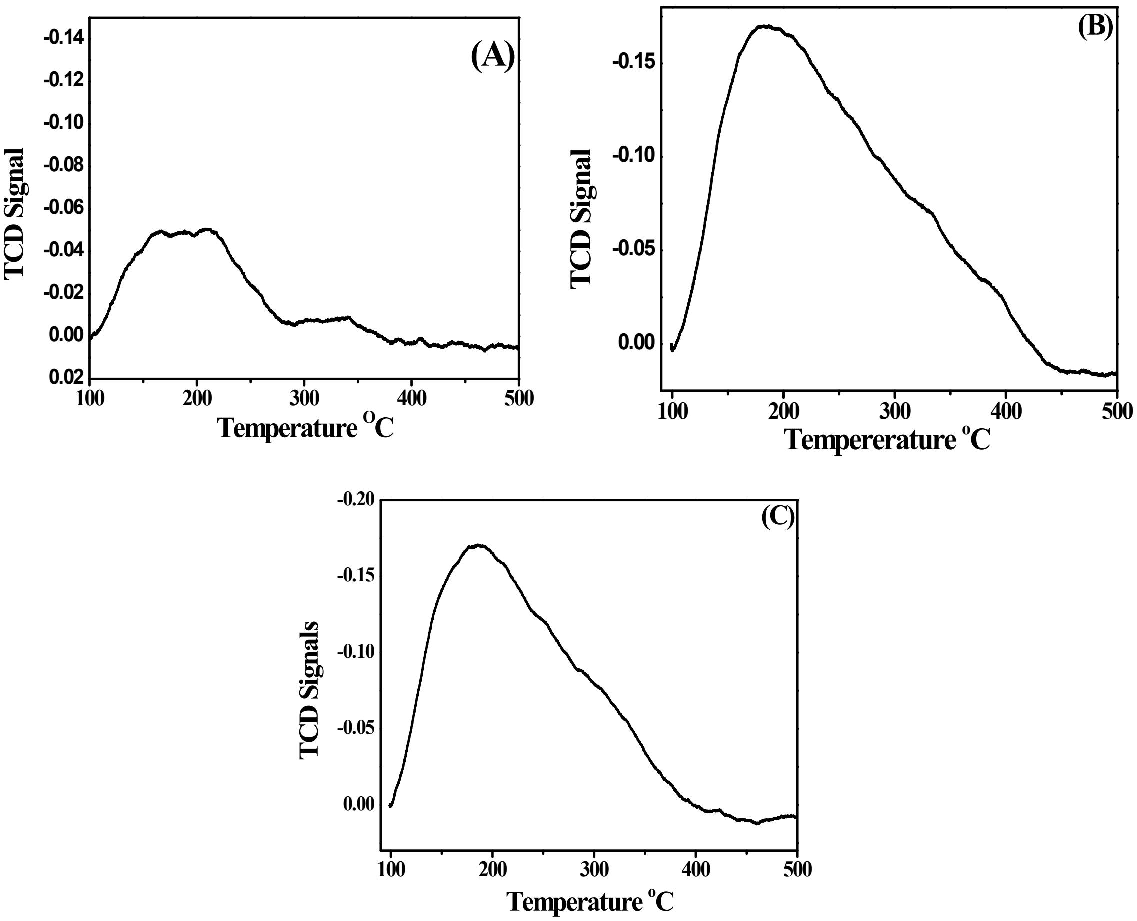

Fig S7-1: NH_3-TPD profile for (A) MoO_3/SiO_2; (B) MoO_3/TiO_2 and (C) MoO_3/ZrO_2

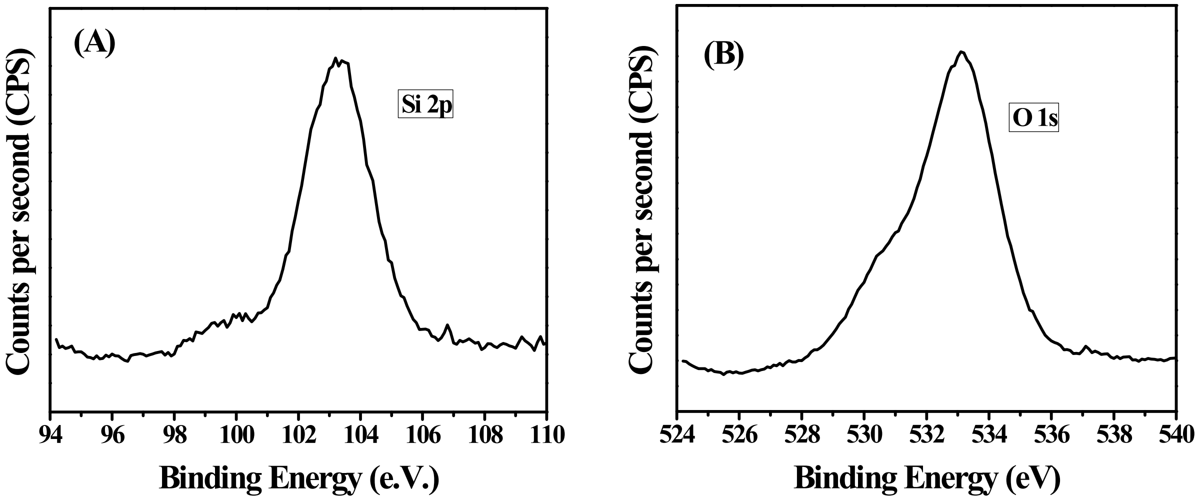

S8- Catalyst characterization by XPS analysis

Fig. S8-1: XPS spectra for (A) Si 2p; (B) O1s of MoO_3/SiO_2 catalyst.

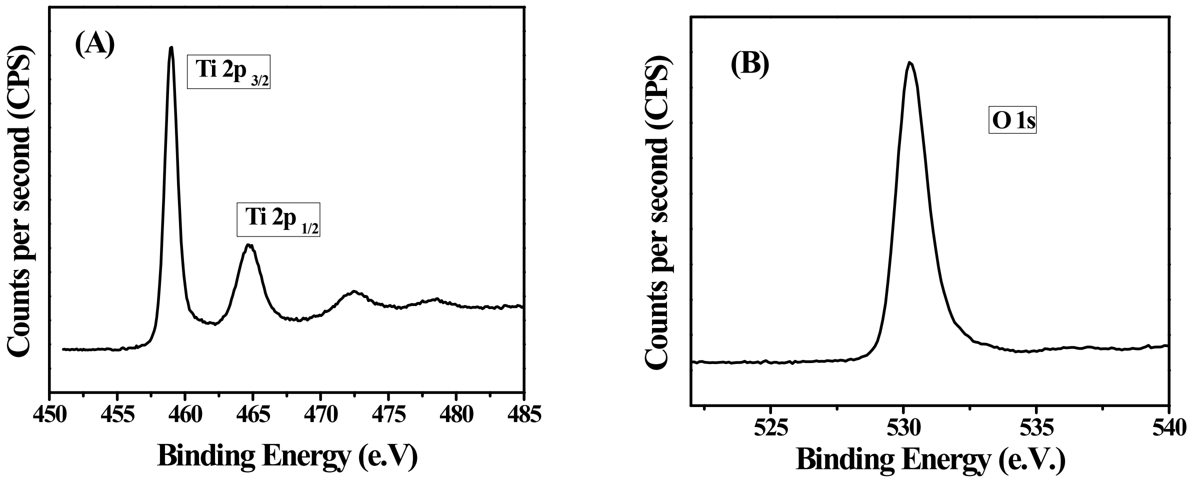

Fig.S8-2: XPS spectra for (A) Ti 2p; (B) O1s of MoO_3/TiO_2 catalyst.

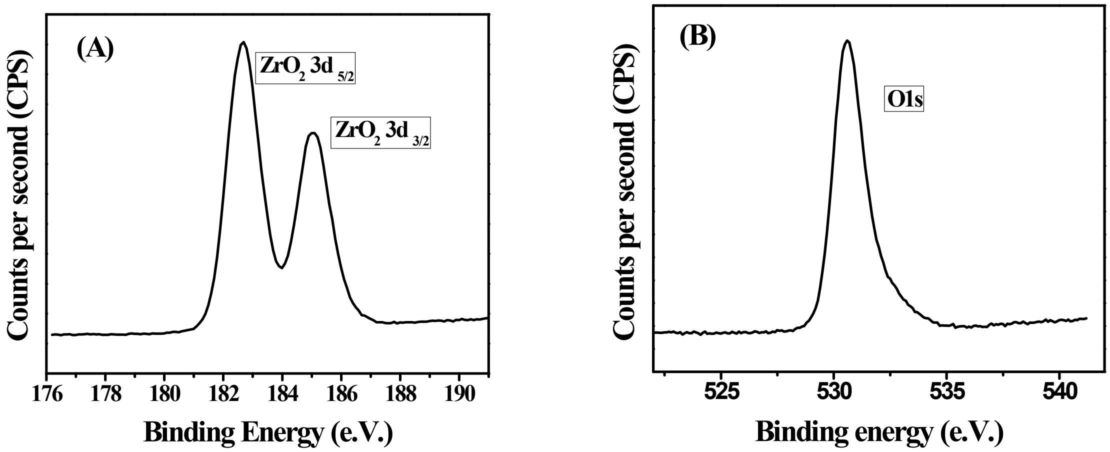

Fig.S8-3: XPS spectra for (A) Zr 3d ; (B) O1s of MoO3/ZrO2 catalyst.

S9: Results of catalytic recycle studies

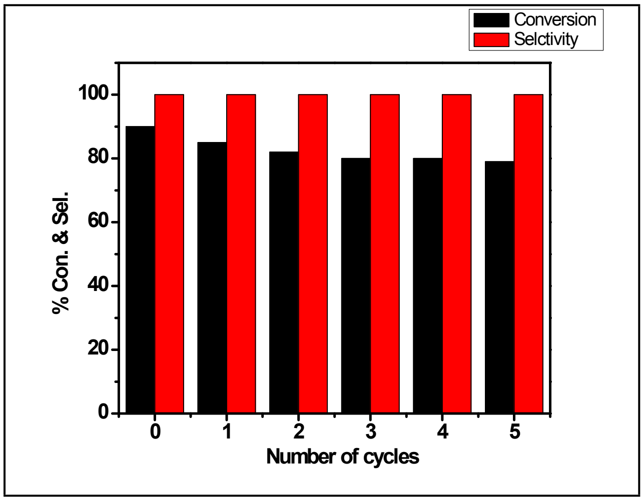

Figure S9: Represents the catalytic recycle study for cyclooctene epoxidation using MoO_3/SiO_2 nanospheres as a catalyst.

Reaction condition: Cyclooctene: 0.285 g (0.0025 mol); Oxidant: (0.0025 mol) 5.5 molar TBHP in decane; Temperature: 80 °C; Solvent: 1,2-dichloroethane (6 g); Catalyst: 0.02 g; Time: 2 h.

S10: TEM analysis of the spent catalyst

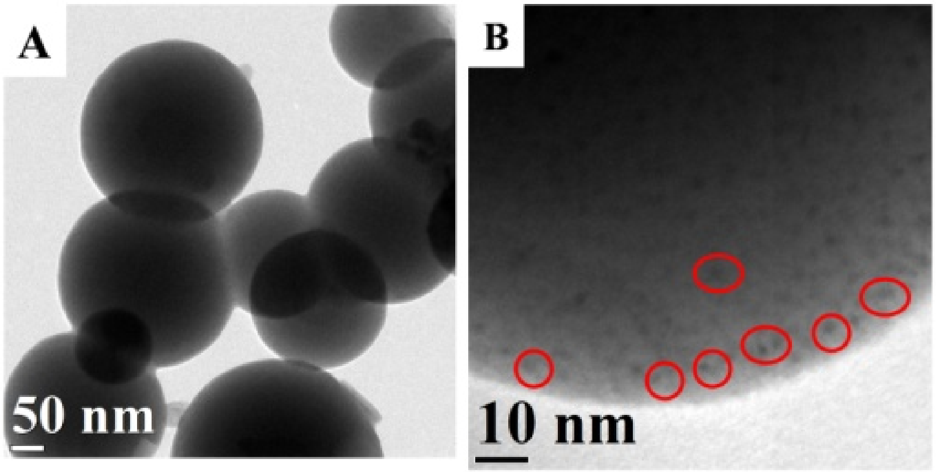

Figure S10: (A and B) represents the HRTEM image of spent catalyst MoO_3/SiO_2 at 50 nm and 10 nm scale.

S11: Catalyst leaching studies by hot filtration Vs blank

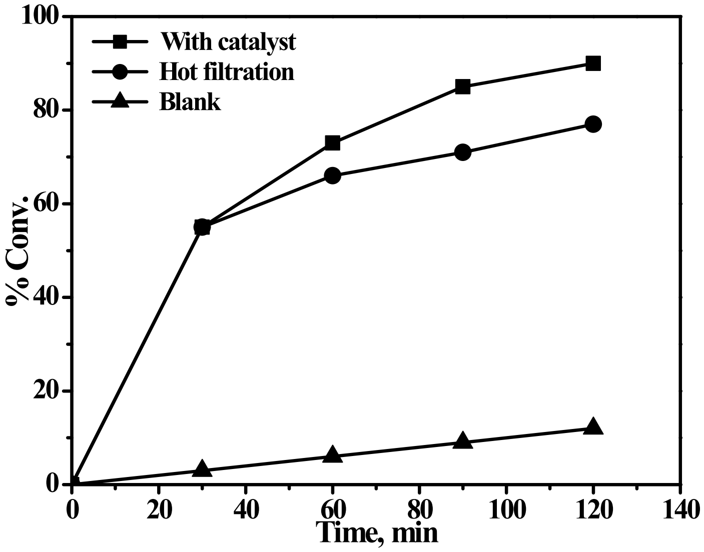

Figure S 11: Represents % cyclooctene conversion vs. time curve; in the catalytic, hot filtration and blank reactions.

Reaction condition: Cyclooctene: 0.282 g (0.0025 mol); Oxidant: (0.0025 mol) 5.5 molar TBHP in decane; Temperature: 80 °C; Solvent: 1, 2-dichloroethane (6 g); Catalyst: 0.02 g; Time-2 h;